RSC Advances

PAPER

View Article Online
View Journal | View Issue

Cite this: *RSC Adv.*, 2017, **7**, 50216

Diethylenetriamine-assisted *in situ* synthesis of TiO_2 nanoparticles on carbon nanotubes with well-defined structure and enhanced photocatalytic performance†

Hailong Peng,[a] Xiaoyan Yang,[b] Peng Zhang,[c] Yiming Zhang,[a] Chengwei Liu,[a] Dan Liu*[a] and Jianzhou Gui*[ac]

A simple diethylenetriamine (DETA)-assisted solvothermal method is utilized for *in situ* synthesis of TiO_2 nanoparticles on carbon nanotubes (CNTs), fabricating TiO_2/CNT composites with well-defined structure and enhanced photocatalytic activity for the degradation of methylene blue (MB). It is found that the DETA plays an important role on the structure, photoelectrochemistry and catalytic performance of the TiO_2/CNT composites. Particularly, the TiO_2/CNT catalyst obtained in the presence of 0.02 mL DETA exhibits both a low adsorption capacity and high photodegrading activity for MB removal under the UV-light irradiation, proving the uniform and well-dispersed TiO_2 particles loaded. Systematic characterization reveals the strong interaction and high electron-transfer efficiency between TiO_2 and CNT in the sample with the assistance of DETA. Besides, a DETA-assisted formation mechanism of the TiO_2/CNT composite has also been proposed in this study: DETA will work as a connecting bridge to facilitate the uniform adsorption of Ti^{4+} on the surface of CNT. With the increase of solvothermal temperature, the adsorbed Ti^{4+} gradually *in situ* crystallizes to form the TiO_2/CNT composite. The DETA-assisted *in situ* synthesis could be expected to be a promising method for the preparation of metal oxides supported on carbon materials with well-defined structure and superior photocatalytic or photoelectrochemical properties.

Received 23rd August 2017
Accepted 17th October 2017

DOI: 10.1039/c7ra09324a

rsc.li/rsc-advances

1. Introduction

Water pollution derived from organic contaminants has recently become a prominent problem that endangers human health, and needs to be solved. Up to now, many approaches have been developed to effectively remove organic pollutions in water, including adsorption,[1,2] biodegradation,[3] and photodegradation.[4–14] Particularly, photodegradation is considered as an ideal treating technology, due to the straightforward process, low energy consumption and high efficiency. Among exciting semiconductor photocatalysts, TiO_2 not only features a low cost, rich resources, and nontoxicity, but also high photocatalytic activity and stability under the irradiation of UV-light, thus attracting tremendous research interest.[15] Even so, the photocatalytic activity of TiO_2 still fails to meet the industrial requirements, thus needing to be significantly improved.

It is found that the hybridization of carbon materials can greatly enhance the photocatalytic activity of TiO_2.[16–20] On the one hand, as catalyst supports, the carbon materials can disperse and anchor TiO_2 particles to exhibit more catalytic active sites. On the other hand, benefiting from the high electrical conductivity, the carbon materials can effectively capture the photogenerated electrons on the surface of TiO_2, prolonging the lifetime of oxidative active species.[21] Among the selectable carbon materials, carbon nanotube (CNT) is regarded as a promising carbon material to be combined with TiO_2, due to the large surface area, strong adsorption effect, and high structural flexibility.[22,23] Baiju K. Vijayan *et al.*[24] utilized a simple hydration/dehydration method to prepare CNT/TiO_2 composites, which show great photocatalytic activity for degradation of acetaldehyde. Taicheng An *et al.*[25] reported that TiO_2 spheres with controllable crystallite size and dominant crystal facets such as {001}, {101}, or polycrystalline were successful supported on CNT, exhibiting the significant synergistic effect and enhanced photocatalytic efficiency. Jing Di *et al.*[26] successfully synthesized plant leaf-shape TiO_2 supported on CNT, which

[a]State Key Laboratory of Separation Membranes and Membrane Processes, College of Environment and Chemical Engineering, Tianjin Polytechnic University, Tianjin 300387, China. E-mail: jzgui@hotmail.com; ldan2000@163.com; Tel: +86-022-83955668

[b]School of Chemistry and Chemical Engineering, Shangqiu Normal University, Shangqiu 476000, China

[c]School of Material Science and Engineering, Tianjin Polytechnic University, Tianjin 300387, China

† Electronic supplementary information (ESI) available. See DOI: 10.1039/c7ra09324a

features not only a large specific surface area, but also a high light absorption due to the great scattering ability. Although some efforts have been devoted in previous works, due to the hydrophobicity, CNT shows a poor dispersity in water[27] and a bad combination with metal cations, making it very difficult to uniformly deposit metal oxide on the surface. Up to now, it is still a big challenge to fabricate the TiO_2/CNT composite photocatalyst with the uniformly loaded and structural controllable TiO_2 particles, as well as the high photocatalytic performance.

Herein, a simple and facile solvothermal method is utilized to prepare TiO_2 nanoparticles supported on CNT with the assistance of DETA. By tuning different precursor (isopropyl titanate, CNT, DETA), a group of TiO_2/CNT composites have been separately obtained, and their adsorption capacity and photodegrading activity for MB removal were evaluated in detail. It is found that DETA greatly affect the loading uniformity and dispersity of TiO_2 particles supported, and the TiO_2/CNT composite with 0.02 mL DETA added shows a strong interaction and the rapid electron-transfer efficiency between TiO_2 and CNT. Moreover, a possible DETA-assisted formation mechanism of the TiO_2/CNT composite has also been proposed in this work.

2. Experimental

2.1 Preparation of a series of the TiO_2/CNT composites

Materials. CNT was provided by Institute of Process Engineering, Chinese Academy of Sciences. Isopropyl alcohol (IA), nitric acid and sulfuric acid were purchased from Fengchuan Chemical Reagent Technologies Co., Ltd. (Tianjin, China), while diethylenetriamine (DETA, 99 wt%) and isopropyl titanate (IT, 97 wt%) were supplied by Macklin Biochemical Co., Ltd. (Shanghai, China).

Preparation of the acid-treated CNT. 5 g CNT, 50 mL deionized (DI) water, 150 mL sulfuric acid (98 wt%) and 50 mL nitric acid (65 wt%) were added in a 500 mL round flask in turn, and magnetically stirred to yield a mixture. After that, this mixture was heated in an oil bath at 100 °C for 4 h. Undergoing washing with DI water up to neutral pH, and drying at 80 °C overnight, the acid-treated CNT was obtained and denoted as o-CNT in this work.

Preparation of a series of TiO_2/CNT composites. The o-CNT was ultrasonically dispersed in 53 mL IA, yielding a suspension. Under magnetically stirring, a certain amount of DETA and IT were slowly added into the resultant suspension, which was transferred into an 80 mL autoclave and maintained at 200 °C for 24 h. After cooled down to room temperature, the solvothermal sample was collected by centrifugation, thoroughly rinse with ethanol, then dried at 60 °C for 24 h. Afterward, the as-obtained product was loaded into a tube furnace, and calcined at 400 °C in air for 2 h with a heating rate of 1 °C min^{-1} to remove the impurities. In the present work, the TiO_2/CNT composites were labeled as z-Ti_xC_y, where x, y, and z refer to the amount of CNT (mg), IT (mL), DETA (mL), respectively, and their corresponding CNT and TiO_2 proportions were listed in Table S1.†

2.2 Characterization of the TiO_2/CNT composites

The morphology of different TiO_2/CNT samples was observed using a scanning electron microscope (SEM, Hitachi S-4800), transmission electron microscope (TEM, Hitachi S-7650) and high-resolution transmission electron microscopy (HRTEM, JEOL JEM-2100). The crystal structure was measured by X-ray diffraction (XRD, Bruker D8 Advance A25, Cu-Kα radiation, 40 kV, 40 mA). The N_2 adsorption–desorption isotherm was tested on Autosorb-iQ-C. X-ray photoelectron spectroscopy (XPS) was carried out on a Thermo Fisher K-Aepra ESCA. The UV-vis diffuse reflectance spectra (DRS) were recorded in a range of 200–800 nm on a Shimadzu UV2700 instrument. Photoluminescence (PL) spectra were measured at room temperature on a fluorescence spectrophotometer (Hitachi F-7000), of which the excitation wavelength was 294 nm.

2.3 Photocatalytic experiments

MB aqueous solution was adopted to evaluate the adsorption capacity and photocatalytic performance of different TiO_2/CNT composites. All the experiments were carried out in a photochemical reactor at room temperature under the ambient situations. In the typical procedure, 0.01 g sample was dispersed in 40 mL MB (20 mg L^{-1}) aqueous solution and magnetically stirred for 30 min in dark to achieve the adsorption/desorption equilibrium. Then, the reaction mixture was exposed to the UV-light, which was provided by a mercury lamp with an average intensity of 150–200 mW cm^{-3}. During the UV-irradiated process, about 4 mL mixture was taken out at intervals of ten minutes, and centrifugated to separate the catalyst from the reaction solution. The resultant filtrate was measured by UV-vis spectrophotometer (Thermo evolution 300). Particularly, the catalytic activity of different samples was evaluated by C/C_0, where C_0 was the MB absorbance of initial solution at 664 nm, and C was the MB real-time absorbance of reaction solution.

Three colorless antibiotics were also used as a target for photodegradation. In the reaction, 0.01 g sample was dispersed in three antibiotics solution (20 mg L^{-1} tetracycline (TC), 20 mg L^{-1} enrofloxacin hydrochloride (ENRH) and 10 mg L^{-1} ciprofloxacin (CIP)) and magnetically stirred for 30 min in dark to achieve the adsorption/desorption equilibrium. And then, the photocatalytic experiment began at the same condition. About 4 mL mixture was taken out per 20 minutes, and then centrifugal separation to obtain the reaction solution. The catalytic activity of different samples was evaluated by C/C_0, where C_0 was the three colorless antibiotics (TC, ENRH and CIP) absorbance of initial solution at 357, 273 and 273 nm, and C was the three colorless antibiotics real-time absorbance of reaction solution.

3. Results and discussions

3.1 Adsorption capacity and photocatalytic activity of different TiO_2/CNT composites

In the present case, two important parameters are adopted to evaluate the structure of TiO_2 particles loaded in the TiO_2/CNT composites: adsorption capacity for MB molecules in dark and

photocatalytic efficiency in the degradation of MB solution under the irradiation of UV-light. As shown in Fig. S1,† the pure CNT exhibits a remarkable MB adsorption, while the commercial TiO_2 sample almost has no adsorption for MB under the same conditions. As for the TiO_2/CNT composites, they should have the decreasing adsorption capacity compared with the pure CNT, due to the CNT surface has been covered by TiO_2 particles. Meanwhile, CNT can rapidly transfer the surface photogenerated electrons to enhance its photocatalytic activity of TiO_2.[19] The detailed adsorption and photocatalysis processes of the TiO_2/CNT composite have been shown in Scheme 1: in dark, the hydrophobicity of CNT will impel MB molecules in solution to be preferentially adsorbed on the bare CNT surface. After exposed to UV-light, TiO_2 particles are excited to produce the electron/hole pairs (reaction a), most of which will rapidly recombine in a very short time (reaction b). Benefiting from the high conductivity, the hybridized CNT can provide a transferred channel to effectively separate the photogenerated electrons (e^-) from the contacted TiO_2 particles. The yielded photogenerated holes (h^+) can oxidize MB molecules to organic intermediates, as shown in Scheme 1 (reaction c). Simultaneously, the photogenerated electrons react with the dissolved oxygen in H_2O to form hydroxyl radicals ($^{\bullet}OH$, reaction d), which has also been proved to be capable to decompose the MB molecules (reaction e). Therefore, in the TiO_2/CNT composite, while the interaction with CNT and dispersity of TiO_2 particles could be evaluated by the improvement of the photocatalytic activity. From Fig. S2,† it should be noted that the self-degradation of MB is too slight to be considered in this work.

A series of TiO_2/CNT composites have been prepared by tuning three precursor amounts, *i.e.* isopropyl titanate (IT), CNT, and DETA. Their theoretical chemical compositions have been summarized in Table S1,† and the adsorption capacity and photocatalytic activity have also been investigated systematically, as shown in Fig. 1.

By changing the weight ratio of TiO_2 from 71% to 91% (Table S1†), the 0.04-Ti_xC_{67} composites generally exhibit the similar MB-removed efficiency, as shown in Fig. 1a. By the plots of $\ln(C/C_0)$ *vs.* illumination time (Fig. 1d), the first-order linear relationship could be found in all the four samples, of which the undistinguishable fitting-line slopes imply the similar photocatalytic activity of the 0.04-Ti_xC_{67} composites. From the relationship between the adsorption and catalytic capability (Fig. 1g), it can be clearly seen that the 0.04-$Ti_{1.2}C_{67}$ shows slightly enhanced catalytic performance compared with others, as well as the remarkably lower adsorption capacity. Obviously, the TiO_2 overloaded in TiO_2/CNT composite may greatly affect the loading uniformity of TiO_2 particles due to their aggregation, whereas exhibiting a negligible difference for their photocatalytic activity.

By increasing CNT amount, the adsorption capacity of corresponding samples firstly decreased and then increased, while their catalytic activity has the reverse trend (Fig. 1b, e and h). As shown in Fig. 1h, when the additive amount of CNT is 67 mg, the 0.04-$Ti_{1.2}C_{67}$ has the lowest adsorption for MB, indicating the highest coverage proportion among these samples. As the CNT content continuously increasing, more TiO_2 active sites will be exposed, resulting in the increasing photocatalytic activity. Therefore, although improving the dispersity of TiO_2 nanoparticles, the increase of CNT content seems not to improve their uniformity simultaneously, which fails to fabricate the TiO_2/CNT composite with well-defined structure.

In addition, DETA in the system also plays an important role in controlling the structure of TiO_2/CNT composite. As shown in Fig. 1c, the MB-removed efficiency of the 0.01-$Ti_{1.2}C_{67}$ and 0.02-$Ti_{1.2}C_{67}$ is much higher than that of the 0-$Ti_{1.2}C_{67}$, mainly owning to their greatly enhanced photocatalytic performance (Fig. 1f). Fig. 1i shows that the two TiO_2/CNT composites have a gradually decreasing adsorption for MB with the DETA amount, indicating that the introduce of DETA can effectively promote the TiO_2 loading uniformity. However, excess DETA, in the case of 0.04-$Ti_{1.2}C_{67}$, inversely leads to the obvious decrease in photocatalytic performance, meanwhile it exhibits the lowest adsorption capacity compared with other samples. Therefore, the appropriate DETA will play an important role in fabricating the TiO_2/CNT composite with both the great TiO_2 loading uniformity and the high dispersity.

Besides MB, the 0.02-$Ti_{1.2}C_{67}$ also exhibits a great photocatalytic performance for the degradation of colorless organics (TC, ENRH, CIP), the reaction processes of three antibiotics have shown in Fig. 2. Obviously, three antibiotics are found to be rapidly degradated over the 0.02-$Ti_{1.2}C_{67}$ under the UV irradiation, which removes almost 99% TC, 94% ENRH and 95% CIP after exposed in UV light for 120 min. It is indicated that the resultant 0.02-$Ti_{1.2}C_{67}$ has a good photocatalytic efficiency for many organic molecules.

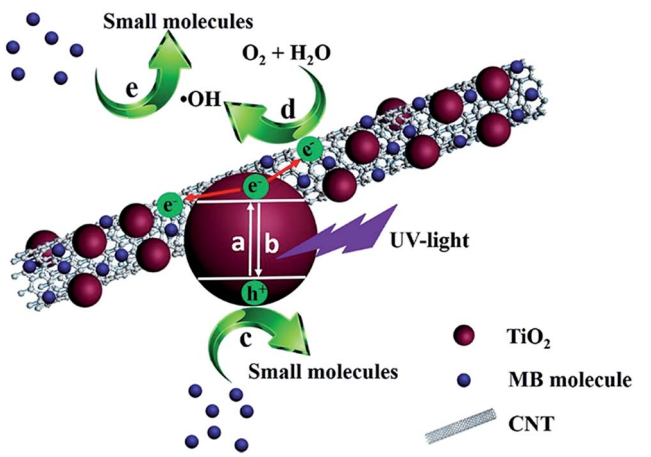

Scheme 1 Adsorption and photocatalytic processes of TiO_2/CNT composite for the MB removal under UV-light irradiation.

3.2 Effect of DETA on the structure of the TiO_2/CNT composite

To figure out the role of DETA, in the present case, the 0-$Ti_{1.2}C_{67}$ and 0.02-$Ti_{1.2}C_{67}$ are chosen and explore the structural difference. Fig. 3a compares the XRD patterns of the 0-$Ti_{1.2}C_{67}$ and 0.02-$Ti_{1.2}C_{67}$, showing the identical diffraction peaks assigned to anatase phase of TiO_2 (JCPDS no. 21-1272).[21,28] It is indicated

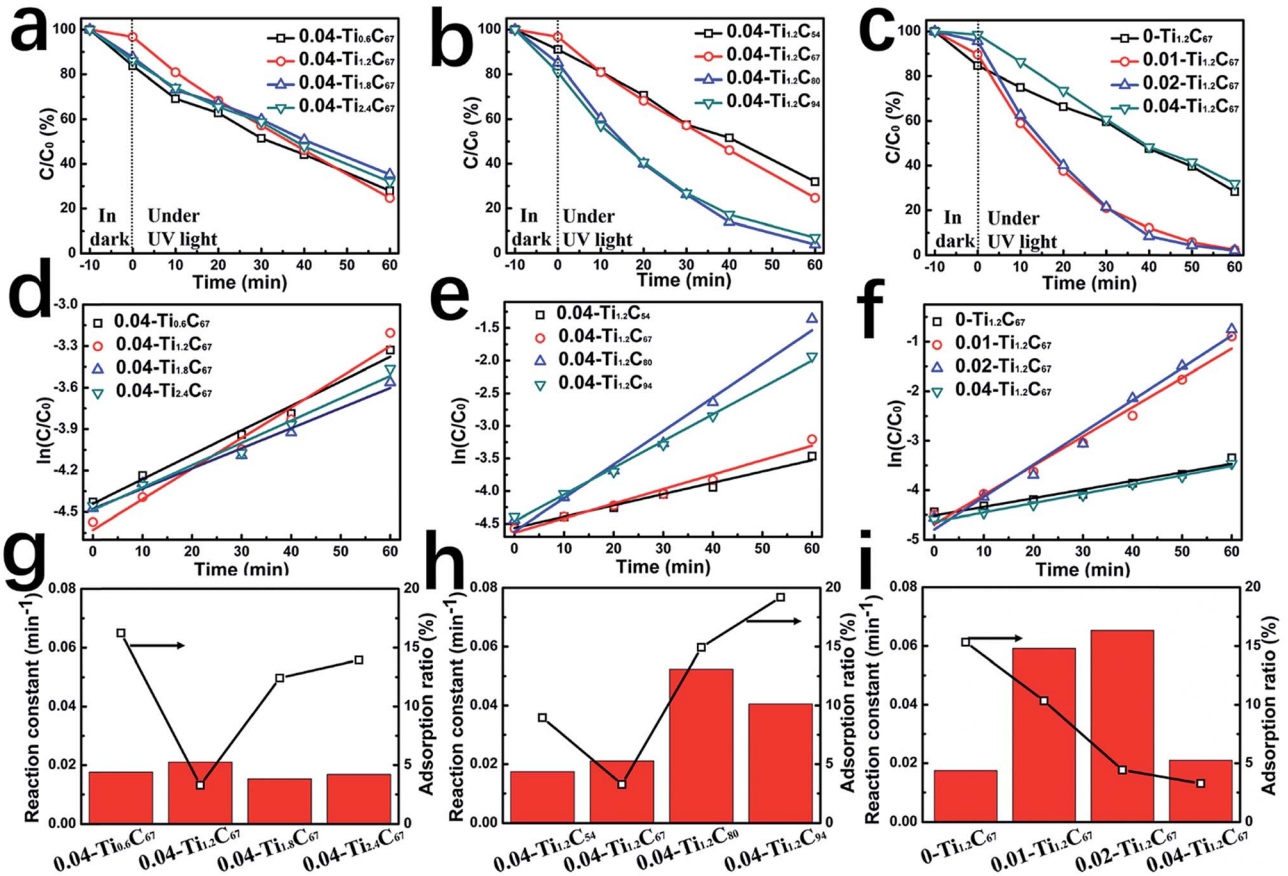

Fig. 1 Photocatalytic decomposition of MB over various TiO_2/CNT composites under UV-light irradiation (a–c); corresponding reaction kinetic curves (d–f); photocatalytic rate constants and adsorption ratio of various TiO_2/CNT composites (g–i).

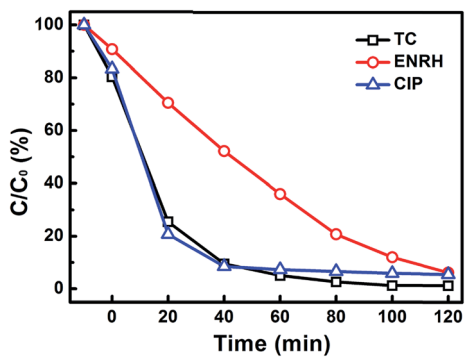

Fig. 2 Photocatalytic degradation of three antibiotics (TC, ENRH, CIP) over 0.02-$Ti_{1.2}C_{67}$ under UV-light irradiation.

that the DETA has no influence on the crystal growth of TiO_2 under the solvothermal situations. It should be noted that no feature peak of CNT can be found in two XRD patterns, which is due to that the diffraction peak of CNT at *ca.* 26° is overlapped with the TiO_2 (101).[21] The structural difference between the 0-$Ti_{1.2}C_{67}$ and 0.02-$Ti_{1.2}C_{67}$ will be further discussed in this paper below. Besides, other TiO_2/CNT samples obtained also have the same crystal compositions with the 0-$Ti_{1.2}C_{67}$ and 0.02-$Ti_{1.2}C_{67}$, resulting from the same XRD patterns (Fig. S3†).

From Fig. 3b, we can clearly see that the 0-$Ti_{1.2}C_{67}$ and 0.02-$Ti_{1.2}C_{67}$ show the coincident N_2 adsorption–desorption isotherms, and their BET surface areas have been estimated to be 138.863 $m^3\ g^{-1}$ and 147.217 $m^3\ g^{-1}$, respectively.

SEM images of the two samples loaded by TiO_2 particles with/without the assistance of DETA (0.02-$Ti_{1.2}C_{67}$ and 0-$Ti_{1.2}C_{67}$) have been shown in Fig. 4a and b, both the two samples have partially maintained the initial wire-type morphology of CNT (Fig. S4†), illustrating that CNT works as the framework in the fabrication of the TiO_2/CNT composite. Particularly, the 0.02-$Ti_{1.2}C_{67}$ displays a highly entangled one-dimensional parasitic architecture with a 40–45 nm diameter size, which is slightly larger than the pure CNT (30–35 nm). On the contrary, a cluster of TiO_2 particles could be clearly observed in the 0-$Ti_{1.2}C_{67}$ (Fig. 4b), through a lot of coarse nanowires are also presented in the appearance. The detailed structure of the two products would be revealed by the corresponding TEM images (Fig. 4c and d). For the sample 0.02-$Ti_{1.2}C_{67}$, TiO_2 particles are evenly grown along the CNT, whereas the 0-$Ti_{1.2}C_{67}$ has both the badly aggregated TiO_2 particles and the bare CNT. From the SEM and TEM images, it is indicated that the TiO_2 loading uniformity of the TiO_2/CNT composite could be significantly improved, when DETA is introduced into the solvothermal system. This structural difference can also be seen from their HRTEM images (Fig. 4e and f). As shown, compared

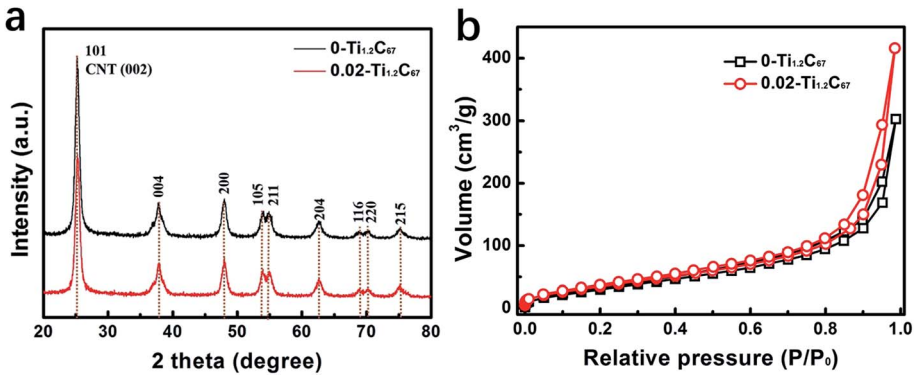

Fig. 3 (a) XRD patterns and (b) N_2 adsorption–desorption isotherms of 0-$Ti_{1.2}C_{67}$ and 0.02-$Ti_{1.2}C_{67}$.

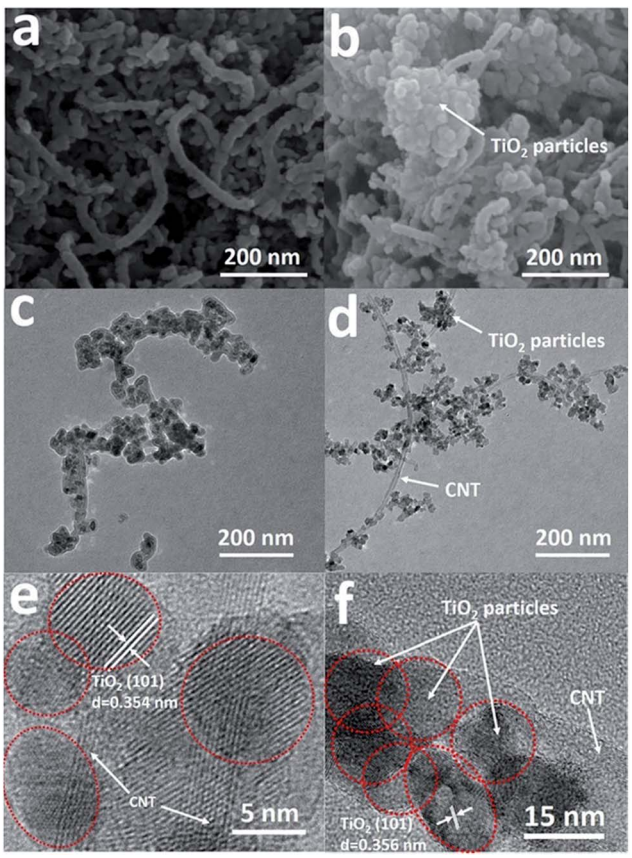

Fig. 4 SEM, TEM and HRTEM images of 0.02-$Ti_{1.2}C_{67}$ (a, c, e) and 0-$Ti_{1.2}C_{67}$ (b, d, f).

with the 0-$Ti_{1.2}C_{67}$, the 0.02-$Ti_{1.2}C_{67}$ possesses the well-dispersed TiO_2 particles on the CNT. Moreover, the clear lattice fringes with interplanar spacing of 0.354 nm and 0.356 nm are found in two HRTEM images, which match well with the TiO_2 (101) lattice plane. Obviously, in spite of the different uniformity and dispersity, TiO_2 particles in two samples (Fig. 4e and f) show a high crystallinity and the same crystal structure.

XPS is conducted to further distinguish the structural difference between the 0.02-$Ti_{1.2}C_{67}$ and 0-$Ti_{1.2}C_{67}$, and the detailed results have been displayed in Fig. 5. From their XPS survey spectra (Fig. 5a), we can see the identical peaks in both XPS spectra, indicating the similar general structure. Besides, the 0.02-$Ti_{1.2}C_{67}$ and 0-$Ti_{1.2}C_{67}$ also exhibit the same high-resolution XPS spectra of Ti (Fig. 5b), in which two bands centered at 458.6 and 464.3 eV correspond to Ti(IV) $2p_{1/2}$ and Ti(IV) $2p_{3/2}$,[29–31] respectively. However, as shown in Fig. 5c, the peak at 532.1 eV assigned to C–O–Ti could be clearly observed in XPS spectrum of O 1s of the 0.02-$Ti_{1.2}C_{67}$, which is much stronger than that of 0-$Ti_{1.2}C_{67}$. This result demonstrates that an interaction excits between CNT and TiO_2 in the 0.02-$Ti_{1.2}C_{67}$. Meanwhile, due to the extensive coverage of TiO_2 particles, there are a lot of oxygen-containing groups reserved on CNT, thus a peak from C–O or C=O (533.5 eV) is also presented in the 0.02-$Ti_{1.2}C_{67}$.[31–33] Consistence with the XPS result of O 1s, the 0.02-$Ti_{1.2}C_{67}$ also has an additive peak at 288.9 eV in the XPS spectrum of C 1s (Fig. 5d), which can be attributed to the Ti–O–C,[34–37] further indicating the strong interaction between TiO_2 and CNT in the 0.02-$Ti_{1.2}C_{67}$. Moreover, the detailed chemical compositions of the 0.02-$Ti_{1.2}C_{67}$ and 0-$Ti_{1.2}C_{67}$ analyzed by XPS have been summarized in Tables S2 and S3,† respectively.

In UV-DRS of the 0-$Ti_{1.2}C_{67}$ and 0.02-$Ti_{1.2}C_{67}$ (Fig. 6a), both a strong absorption in UV region (below 400 nm) and visible absorption in 400–800 nm could be observed, while the 0.02-$Ti_{1.2}C_{67}$ shows a stronger visible absorption compared with the 0-$Ti_{1.2}C_{67}$, probably because of its high dispersity of TiO_2 particles on CNT. However, from the plots of $(\alpha h\nu)^2$ *versus* $(h\nu)$,[38] we can find no obvious difference between the band gap energy (E_g) of 0-$Ti_{1.2}C_{67}$ and 0.02-$Ti_{1.2}C_{67}$, indicating no effect of DETA on the band gap of TiO_2/CNT composites.

PL is a powerful tool to analyze the essential optical property of photocatalysts. Fig. 7 compares PL spectra of the 0-$Ti_{1.2}C_{67}$ and 0.02-$Ti_{1.2}C_{67}$ at an excitation wavelength of 294 nm, both of which include an emission peak at *ca.* 396 nm and series of peaks in the range of 440–500 nm. Generally, the strong peak at *ca.* 396 nm is attributed to the electron transition of the bandgap energy of anatase TiO_2 (~397 nm),[39,40] while peaks ranging from 440 to 500 nm are ascribed to the electron migration resulted from the surface defects.[41] For the 0.02-$Ti_{1.2}C_{67}$, the quenching fluorescence indicates a faster transfer of surface electrons than the 0-$Ti_{1.2}C_{67}$, resulting from the close contact between TiO_2 and CNT. Therefore, the 0.02-$Ti_{1.2}C_{67}$ has

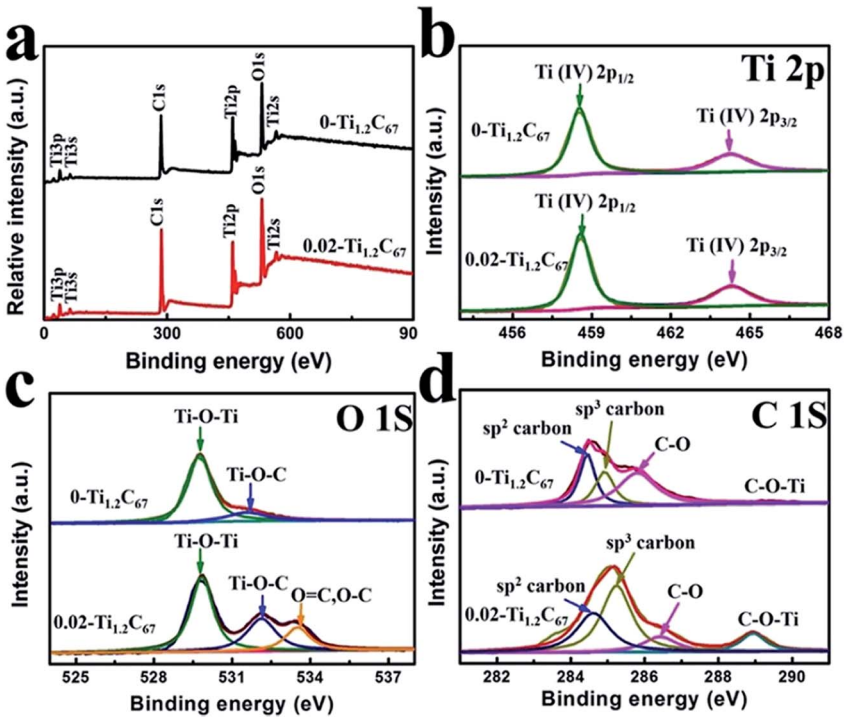

Fig. 5 (a) XPS survey spectra of 0.02-$Ti_{1.2}C_{67}$ and 0-$Ti_{1.2}C_{67}$; high-resolution XPS spectra of (b) C 1s; (c) O 1s; (d) Ti 2p of 0.02-$Ti_{1.2}C_{67}$ and 0-$Ti_{1.2}C_{67}$.

exhibited the superior photocatalytic activity in the photodegradation of MB under the irradiation of UV-light. Meanwhile, the equivalent emission peaks from 440–500 nm can be clearly seen in two samples, indicating the similar TiO_2 surface structure, which is very agreement with the XPS result discussed above. PL analysis of all samples obtained in this work (Fig. S5†), it is found the CNT and DETA play an important role on the electron transport efficiency of the TiO_2/CNT composites, which well matches with the photocatalytic experimental results. However, the decreasing PL emission peak probably attribute to the increasing amount of CNT in samples. As for *z*-$Ti_{1.2}C_{67}$ samples, a declining PL peak has been observed in the 0.02-$Ti_{1.2}C_{67}$, indicating that when the additive amount of DETA is 0.02 mL, the corresponding product possesses the higher electron-transfer rate from TiO_2 particles to CNT.

Furthermore, the photoelectrochemical property of two TiO_2/CNT composites are investigated by their photocurrent responses and EIS, and the detailed results have been displayed in Fig. 8. From Fig. 8a, we can clearly see that both the 0-$Ti_{1.2}C_{67}$ and 0.02-$Ti_{1.2}C_{67}$ have transient photocurrent responses in three on–off cycles of UV-light irradiation in 0.1 M Na_2SO_4 solution, resulting from the separation of photogenerated electron/hole pairs in two samples. In comparison to the 0-$Ti_{1.2}C_{67}$, the photocurrent density of the 0.02-$Ti_{1.2}C_{67}$ is much higher, demonstrating an increasing electron-transfer efficiency. Consequently, in the 0.02-$Ti_{1.2}C_{67}$, the close contact between TiO_2 and CNT successfully facilitates the migration efficiency of surface electrons. Meanwhile, both the 0.02-Ti_xC_{67} and 0.02-$Ti_{1.2}C_y$ samples have the similar photocurrent intensity, as shown in Fig. S6.† It is demonstrated that the electron-

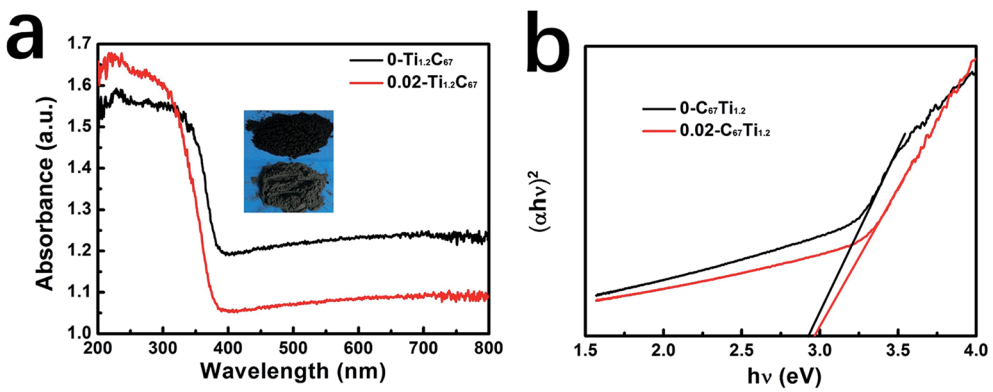

Fig. 6 UV-DRS spectra of 0-$Ti_{1.2}C_{67}$ and 0.02-$Ti_{1.2}C_{67}$.

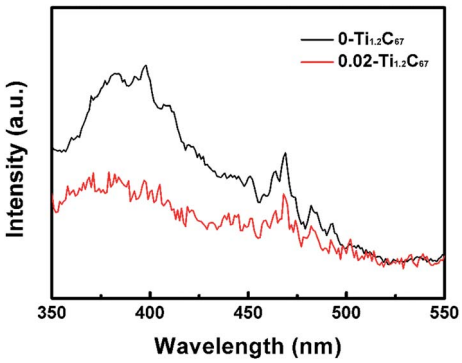

Fig. 7 PL spectra of the 0-$Ti_{1.2}C_{67}$ and 0.02-$Ti_{1.2}C_{67}$ at an excitation wavelength of 294 nm.

migration efficiency of TiO_2/CNT composites cannot be greatly affected by the amounts of CNT and TiO_2 particles in system. On the contrary, DETA is the major influence factor to the materials which can be seen from the great difference photocurrent response.

To further analyze the surface charge migration, EIS of the 0-$Ti_{1.2}C_{67}$ and 0.02-$Ti_{1.2}C_{67}$ were measured in 0.1 M Na_2SO_4 solution, both in dark and under the irradiation of UV-light. For photocatalysts, the Nyquist plot recorded in dark can represent their intrinsic charge-transfer resistance. From Fig. 8b, the identical Nyquist plot in dark indicates that the 0-$Ti_{1.2}C_{67}$ and 0.02-$Ti_{1.2}C_{67}$ have the similar CNT and TiO_2 contents. After exposed to UV-light, the charge migration rate of the two samples have been dramatically accelerated, thus showing two depressed semicircles in the corresponding Nyquist plots. Particularly, the 0.02-$Ti_{1.2}C_{67}$ has the smaller radius than the 0-$Ti_{1.2}C_{67}$, verifying a higher charge migration efficiency. Consequently, the photoelectrochemical result agrees fairly well with the photocatalytic performance of the 0-$Ti_{1.2}C_{67}$ and 0.02-$Ti_{1.2}C_{67}$.

3.3 Growth mechanism of the CNT/TiO_2 composite

In terms of the available information, a possible mechanism has been proposed to figure out the role of DETA for the formation of the TiO_2/CNT composite, as shown in Scheme 2. The whole preparation process of the TiO_2/CNT composite can be probably divided into three steps: (a) first, due to the oxygen-containing functional groups, the acid-treated CNT can effectively combine with $-NH_2$ in DETA *via* physisorption or electrostatic adsorption.[42] (b) Afterwards, the unbinding $-NH_2$ in the DETA-modified CNT further capture dissociated Ti^{4+} ions in

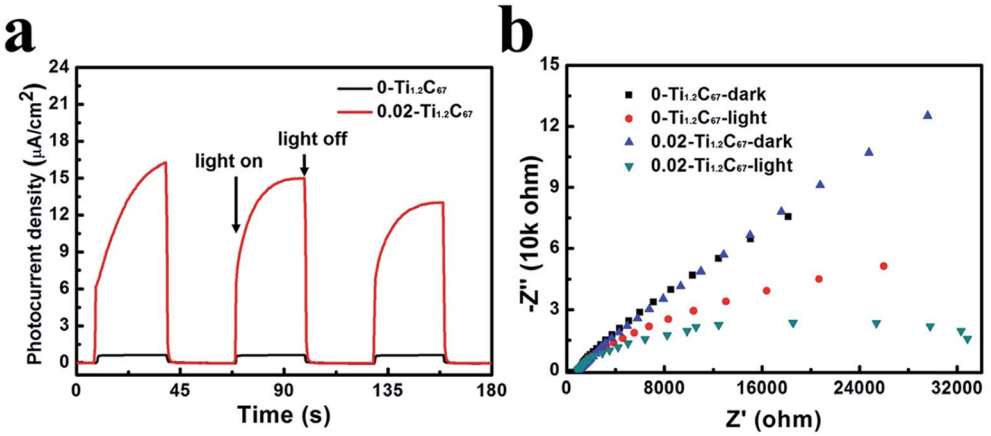

Fig. 8 Photocurrent responses (a) and Nyquist plots (b) of 0-$Ti_{1.2}C_{67}$ and 0.02-$Ti_{1.2}C_{67}$ in 0.1 M Na_2SO_4 solution under UV-light irradiation.

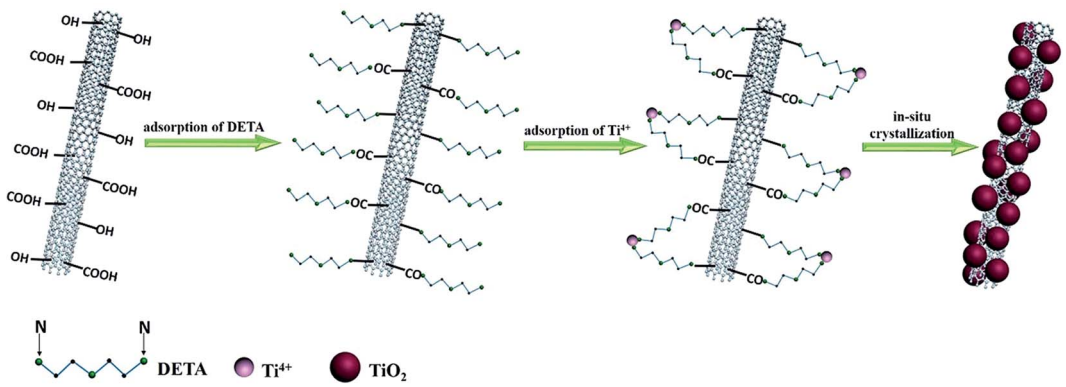

Scheme 2 Possible formation process of the TiO_2/CNT composite in the presence of DETA.

solution to form the catalyst precursor, Ti^{4+}-DETA-CNT.[42,43] (c) As the hydrothermal temperature gradually increases, Ti^{4+} on the precursor will crystallize to yield TiO_2 nanoparticles, which are *in situ* deposited on the surface of DETA-modified CNT. Finally, after thermally treating at the high temperature, DETA and functional groups on the CNT surface are removed, and the TiO_2/CNT composite with the uniformly-loaded and well-dispersed TiO_2 nanoparticles has been successfully prepared.

4. Conclusions

In summary, series of TiO_2/CNT composites have been synthesized *via* tuning the amount of various precursors (IT, CNT, and DETA) under the solvothermal situations. After investigated their adsorption capacity and photodegrading activity under the UV-light irradiation for MB removal, it is found that DETA in synthesis system can remarkably improve the photocatalytic activity of samples, meanwhile decreasing the adsorption amount for MB molecules. Particularly, the 0.02-$Ti_{1.2}C_{67}$ exhibits both the uniformly-loaded TiO_2 nanoparticles on the surface, the high electrons-transfer efficiency and strong interaction between TiO_2 and CNT. Furthermore, a possible DETA-assisted mechanism has been proposed to explain the *in situ* formation of TiO_2/CNT composite, which could develop to be a general method for preparating of metal oxide/carbon (MO/C) composites with the well-defined structure and superior photocatalytic or photoelectrochemical properties.

Conflicts of interest

No conflicts of interest.

Acknowledgements

This work was partly supported by the National Natural Science Foundation of China (No. 21576211 and No. 21706190).

References

1 F. M. Machado, S. A. Carmalin, E. C. Lima, S. L. P. Dias, L. D. T. Prola, C. Saucier, I. M. Jauris, I. Zanella and S. B. Fagan, *J. Phys. Chem. C*, 2016, **120**, 18296–18306.
2 D. Li, Q. Li, N. Bai, H. Dong and D. Mao, *ACS Sustainable Chem. Eng.*, 2017, **5**, 5598–5607.
3 M. Ahmad, S. Liu, N. Mahmood, A. Mahmood, M. Ali, M. Zheng and J. Ni, *ACS Appl. Mater. Interfaces*, 2017, **9**, 13188–13200.
4 P. Zhang, M. Fujitsuka and T. Majima, *Appl. Catal., B*, 2016, **185**, 181–188.
5 W. Jiang, Y. Liu, J. Wang, M. Zhang, W. Luo and Y. Zhu, *Adv. Mater. Interfaces*, 2016, **3**, 1500502.
6 K. Fujiwara, Y. Kuwahara, Y. Sumida and H. Yamashita, *Langmuir*, 2017, **33**, 288–295.
7 Z. Chen, N. Zhang and Y.-J. Xu, *CrystEngComm*, 2013, **15**, 3022.
8 Z. Bian, T. Tachikawa, P. Zhang, M. Fujitsuka and T. Majima, *J. Am. Chem. Soc.*, 2014, **136**, 458–465.
9 D. Yang, H. Liu, Z. Zheng, Y. Yuan, J.-cai Zhao, X. K. Eric, R. Waclawik and H. Zhu, *J. Am. Chem. Soc.*, 2009, **131**, 17885–17893.
10 J. Liu, J. Ke, D. Li, H. Sun, P. Liang, X. Duan, W. Tian, M. O. Tadé, S. Liu and S. Wang, *ACS Appl. Mater. Interfaces*, 2017, **9**, 11678–11688.
11 C. Li, Y. Tang, B. Kang, B. Wang, F. Zhou, Q. Ma, J. Xiao, D. Wang and J. Liang, *Sci. China, Ser. E: Technol. Sci.*, 2007, **50**, 279–289.
12 Y. Dong, D. Tang and C. Li, *Appl. Surf. Sci.*, 2014, **296**, 1–7.
13 Z. Lu, X. Xiang, L. Zou and J. Xie, *RSC Adv.*, 2015, **5**, 42580–42586.
14 Q. Zeng, H. Li, H. Duan, Y. Guo, X. Liu, Y. Zhang and H. Liu, *RSC Adv.*, 2015, **5**, 13430–13436.
15 Y. Ma, X. Wang, Y. Jia, X. Chen, H. Han and C. Li, *Chem. Rev.*, 2014, **114**, 9987–10043.
16 N. Zhang and Y.-J. Xu, *CrystEngComm*, 2016, **18**, 24–37.
17 N. Zhang, M.-Q. Yang, S. Liu, Y. Sun and Y.-J. Xu, *Chem. Rev.*, 2015, **115**, 10307–10377.
18 P. Zhang, B. Li, Z. Zhao, C. Yu, C. Hu, S. Wu and J. Qiu, *ACS Appl. Mater. Interfaces*, 2014, **6**, 8560–8566.
19 P. Zhang, Y. Chen, X. Yang, J. Gui, Y. Li, H. Peng, D. Liu and J. Qiu, *Langmuir*, 2017, **33**, 4452–4460.
20 K. Dai, X. Zhang, K. Fan, T. Peng and B. Wei, *Appl. Surf. Sci.*, 2013, **270**, 238–244.
21 J. Yu, T. Ma and S. Liu, *Phys. Chem. Chem. Phys.*, 2011, **13**, 3491–3501.
22 A. Shayesteh Zeraati, S. A. Mirkhani and U. Sundararaj, *J. Phys. Chem. C*, 2017, **121**, 8327–8334.
23 V. H. Nguyen, C. Kang, C. Roh and J.-J. Shim, *Ind. Eng. Chem. Res.*, 2016, **55**, 7338–7343.
24 B. K. Vijayan, N. M. Dimitrijevic, D. Finkelstein-Shapiro, J. Wu and K. A. Gray, *ACS Catal.*, 2012, **2**, 223–229.
25 T. An, J. Chen, X. Nie, G. Li, H. Zhang, X. Liu and H. Zhao, *ACS Appl. Mater. Interfaces*, 2012, **4**, 5988–5996.
26 J. Di, S. Li, Z. Zhao, Y. Huang, Y. Jia and H. Zheng, *Chem. Eng. J.*, 2015, **281**, 60–68.
27 X. Li, H. Lu, Y. Zhang and F. He, *Chem. Eng. J.*, 2017, **316**, 893–902.
28 J. Zhang, M. Vasei, Y. Sang, H. Liu and J. P. Claverie, *ACS Appl. Mater. Interfaces*, 2016, **8**, 1903–1912.
29 Y. Y. Lu, Y. Y. Zhang, J. Zhang, Y. Shi, Z. Li, Z. C. Feng and C. Li, *Appl. Surf. Sci.*, 2016, **370**, 312–319.
30 H. Zhao, M. Wu, J. Liu, Z. Deng, Y. Li and B.-L. Su, *Appl. Catal., B*, 2016, **184**, 182–190.
31 L. Zhao, X. Chen, X. Wang, Y. Zhang, W. Wei, Y. Sun, M. Antonietti and M. M. Titirici, *Adv. Mater.*, 2010, **22**, 3317–3321.
32 B. Li, Z. Zhao, F. Gao, X. Wang and J. Qiu, *Appl. Catal., B*, 2014, **147**, 958–964.
33 E. Bailón-García, A. Elmouwahidi, M. A. Álvarez, F. Carrasco-Marín, A. F. Pérez-Cadenas and F. J. Maldonado-Hódar, *Appl. Catal., B*, 2017, **201**, 29–40.
34 K. M. Cho, K. H. Kim, H. O. Choi and H.-T. Jung, *Green Chem.*, 2015, **17**, 3972–3978.
35 X. Fan, C. Yu, J. Yang, Z. Ling and J. Qiu, *Carbon*, 2014, **70**, 130–141.

36 X. Fan, C. Yu, Z. Ling, J. Yang and J. Qiu, *ACS Appl. Mater. Interfaces*, 2013, **5**, 2104–2110.
37 S. Liu, C. Liu, W. Wang, B. Cheng and J. Yu, *Nanoscale*, 2012, **4**, 3193.
38 S. Sadhu and P. Poddar, *J. Phys. Chem. C*, 2014, **118**, 19363–19373.
39 Y. T. Liang, B. K. Vijayan, O. Lyandres, K. A. Gray and M. C. Hersam, *J. Phys. Chem. Lett.*, 2012, **3**, 1760–1765.
40 M. Cao, P. Wang, Y. Ao, C. Wang, J. Hou and J. Qian, *Chem. Eng. J.*, 2015, **264**, 113–124.
41 Z. Bian, T. Tachikawa, W. Kim, W. Choi and T. Majima, *J. Phys. Chem. C*, 2012, **116**, 25444–25453.
42 Y.-X. Zhang, X. Guo, X. Zhai, Y.-M. Yan and K.-N. Sun, *J. Mater. Chem. A.*, 2015, **3**, 1761–1768.
43 H. Jianfeng, W. Dan, Y. Lixiong, C. Liyun, O. Haibo, L. Jiayin and H. Wei, *J. Alloys Compd.*, 2014, **612**, 233–238.